

Domain Formation in Model Membranes: Insight from MD Simulations

Patrick Kelley

Prof. Stephen Wassall

1. Introduction

Communication between biological cells and with the organelles in a cell is controlled by the membranes that enclose them. They are composed of lipids and proteins [1]. Lipid molecules with a hydrophilic headgroup and a pair of hydrophobic chains form a bilayer roughly 4 nm thick (Figure 1). Proteins are embedded within or are attached peripherally to the bilayer. There are many kinds of lipid that differ in molecular structure and affinity for each other, which drives lateral segregation into compositionally distinct domains creating the local environment necessary for the function of resident proteins. Lipid rafts are the most studied example [2]. They are domains enriched in sphingolipids and cholesterol molecules tightly packed together that are envisaged as floating in a more loosely packed sea of surrounding lipid. When clustered together, the lipid raft concept posits, the signaling proteins within these nano-sized domains are triggered.

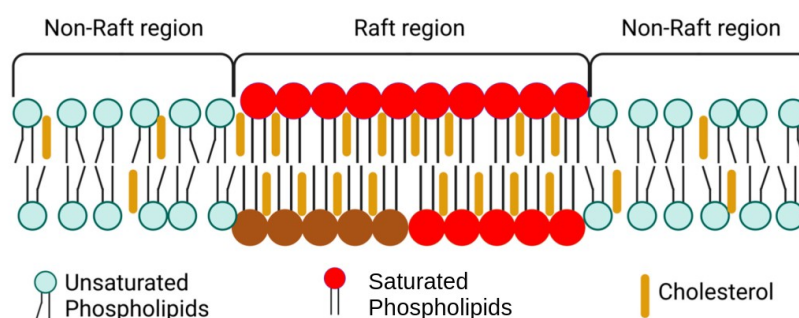


Figure 1: Cartoon of membrane showing raft and non-raft domains. Modified from [3].

This report outlines projects in various stages of progress using coarse-grained (CG) molecular dynamics (MD) simulations to investigate the role that the molecular structure of lipid chains and head groups play in the formation of domains in protein-free model

membranes of well-defined composition. Their immediate aim is to provide insight into the interpretation of results obtained by solid state ^2H NMR and other experimental methods. The aim ultimately is to relate molecular structure of lipids to biological function.

2. Lipid Structure

The lipids that comprise cell membranes are diverse in structure [1]. Three lipids commonly found in biological membranes that serve as a benchmark in this work are 1-palmitoyl-2-oleoylphosphatidylcholine (POPC), palmitoyl sphingomyelin (PSM) and cholesterol (CHOL) (Figure 2). POPC is a glycerophospholipid composed of glycerol backbone to which saturated palmitic (16:0) acid and monounsaturated oleic (18:1) chains are attached at the *sn*-1 and -2 positions, respectively, and a phosphatidylcholine (PC) head group is attached at the *sn*-3 position. PSM is a sphingophospholipid consisting of a sphingosine backbone to which a palmitic acid chain is amide linked. A tetracyclic steroid moiety with a hydroxyl group at one end that typically locates at the surface of a membrane and a short hydrocarbon chain at the other end that extends toward the center comprises CHOL. The rigid steroid moiety is compatible with the largely linear conformation adopted by the predominantly saturated sphingosine and palmitic acid chains in PSM, facilitating close packing and promoting the formation of rafts [2].

Acyl chain structure

A major focus of our research is molecular organization in lipid bilayers containing 1-palmitoyl-2-docosahexaenoylphosphatidylcholine (PDPC). PDPC with docosahexaenoic acid (DHA) at the *sn*-2 position (Figure 2) is representative of a membrane phospholipid into which omega-3 polyunsaturated fatty acids (n-3 PUFA) consumed in fish oils incorporate. The motivation is to understand the origin of the many health benefits associated with fish

oils [4]. Regulation of the size of lipid rafts is a possible mechanism [5]. The basic idea is multiple double bonds, six in the case of DHA (22:6), in a recurring =C-C-C= motif confer tremendously high disorder on PUFA chains. High disorder is incompatible with close proximity to CHOL, which is driven into the more ordered environment within rafts and tunes their size. Simulations run on bilayers composed of PSM, CHOL with POPC and PDPC supporting this model will be presented in this report.

Vitamin E is an essential micronutrient [6]. Alpha-tocopherol (α toc) is the form retained by the human body. The structure of this lipid soluble antioxidant consists of a chromanol ring with a hydroxyl group and a branched phytyl chain at opposite ends (Figure 2). The hydroxyl group usually sits near the surface a membrane while the chain extends into the interior [7]. Due to the presence of multiple double bonds, polyunsaturated lipids are highly susceptible to free radical attack. The role of α toc to protect them from oxidative damage, which means α toc and PUFA chain must meet to terminate a cascade of reactions by which lipid peroxidation proceeds once initiated by a reactive oxygen species [8]. Preliminary simulations that are underway will test the proposal that α toc and polyunsaturated PDPC colocalize together to optimize protection [9] will also be presented in this report.

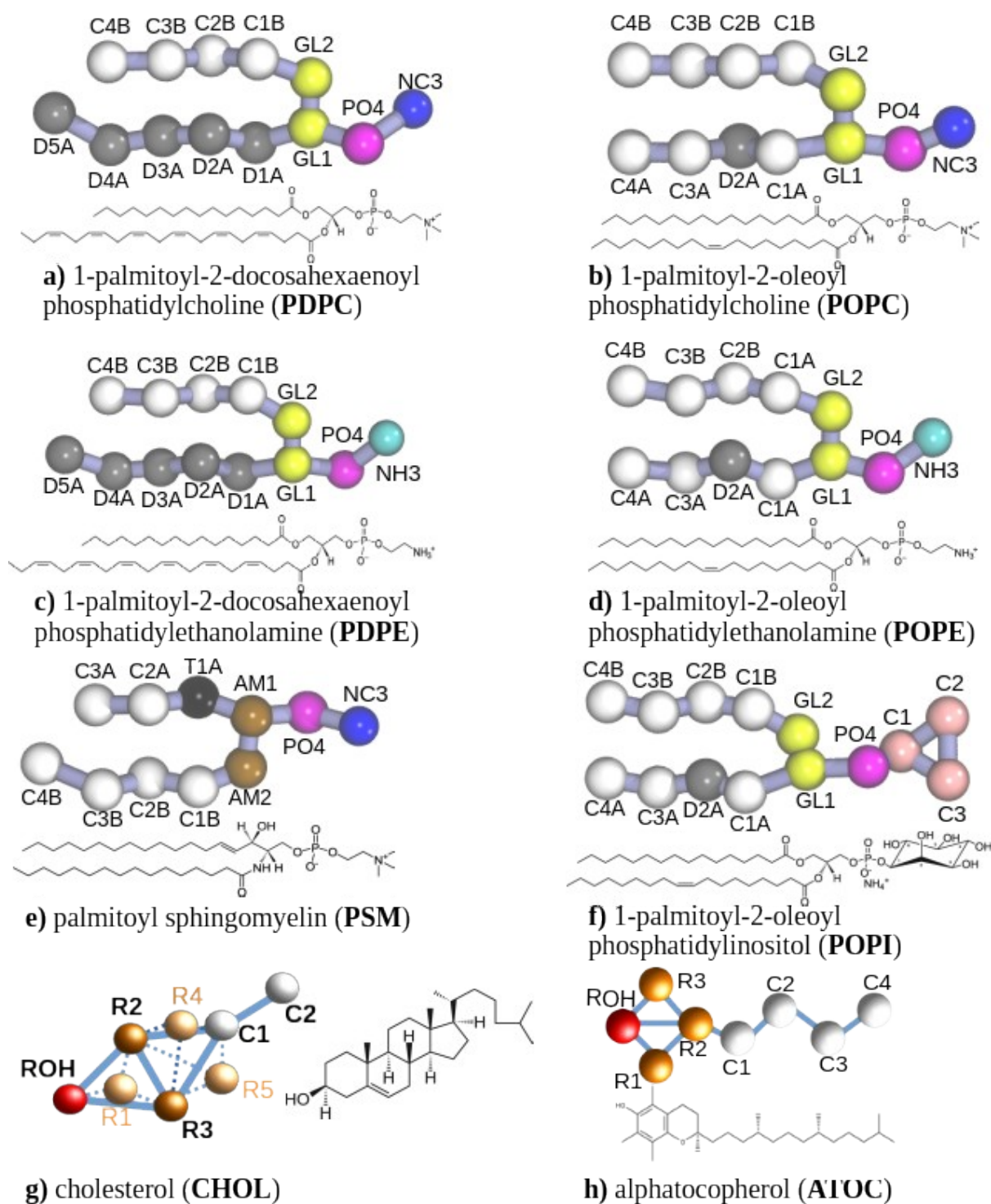


Figure 2: Molecular structure of lipids and corresponding Martini model.

Head group structure

There are also differences in the structure of head groups that affect the interactions between lipids and their segregation into domains in membranes. Two projects are planned involving phosphatidylethanolamine (PE), which after PC is the most common head group on glycerophospholipids [1]. Simulations on mixtures of PSM and CHOL with 1-palmitoyl-2-docosahexaenoylphosphatidylethanolamine (PDPE) (Figure 2) will be compared with its PC counterpart, PDPC, in the first project. The objective is to determine why the smaller size of the PE head group leads to the reduction in domain size with PDPE inferred from ^2H NMR spectra obtained with deuterium substituted analogs of the lipids [10]. In the second project, the interaction between PE and lipids with a phosphatidylinositol (PI) head group (Figure 2) will be investigated. SAXS indicates PE lipids promote the clustering of PI into domains, which serve as the platform for the angiomotin family of proteins that regulates cellular polarity, growth and migration [11].

3. Methods

MD simulations, supplemented by ^2NMR experiments, is the primary method in this work.

3.1 MD simulations

We calculate the trajectories of the atoms on the lipid molecules in a bilayer according to Newton's laws in MD simulations. To allow the study of larger systems over longer timescales, we employed the CG Martini force field [12].

Martini force field

The purpose of Martini is to characterize the most atoms into as few parametrized groups that retain the overall chemical features. A building block approach is applied. Four

consecutively bonded atoms with all corresponding bonded, branched atoms such as hydrogen are described by a single unit called a bead. The ‘force field’ includes intramolecular and intermolecular interactions between beads. Intramolecular forces between bonded beads include harmonic bond and angle potentials, and proper and improper dihedral torsion potentials. Additionally, each individual bead parametrizes the chemical unit in terms of one of four non-bonded intermolecular classes of interaction: polar, nonpolar, intermediately polar, or charged. The polar and nonpolar classes of bead interact only through the Lennard-Jones (LJ) potential. Charged beads include the Coulomb potential. Additionally, the charged or intermediately polar beads include hydrogen bonding capabilities that accounted for by increasing the strength of interaction the LJ potential between certain bead classes.

Martini thus reduces a complicated molecule down into these 18 bead types, denoted as regular (“R”) beads. There are exceptions. Ring-like structures, such as in cholesterol, are described by a small (“S”) bead that use 3-to-1 mapping to better parameterize the chemical nature than the regular 4-to-1-mapped beads.

MD simulation

The first step in our simulations was to assemble and equilibrate a bilayer composed of about 1000 lipid molecules hydrated with around 10,000 water molecules [13]. Production runs were then performed with a time step of typically 30 fs for several μ s in the constant particle number, pressure and temperature (NPT) ensemble using the GROMACS MD package [14].

Domain determination algorithm

A method to distinguish domains based on the lateral density of lipid species in each leaflet of the bilayer in was developed. PSM-rich/CHOL-rich raft-like domains have been our

focus to date. The assignment was made by applying a sliding window method to individual snapshots. A window $\sim 2.6 \times 2.6$ nm (containing on average 11 lipids) in size was tracked ~ 0.9 nm (average separation between lipid molecules) in each direction. Windows for which the count of PSM and Chol exceeds the threshold for random mixing with a 75% probability were designated raft-like. Windows were deemed to be non-raft otherwise. The domain type for each $\sim 0.9 \times 0.9$ nm² area was assigned and tallied 9 separate times by the sliding window, and ultimately classified by majority vote. The lipids inside the area were correspondingly categorized.

3.2 ²H NMR

The MD simulations complement our detection of domains by solid state ²H NMR employing deuterated analogs of lipids - usually perdeuterated throughout an entire chain [15]. The ²H nucleus (spin 1) possesses a quadrupolar moment that interacts with the electric field gradient (EFG) stemming from the directly bonded carbon in a lipid chain. This coupling perturbs the Zeeman interaction when a magnetic field is applied, separating the NMR signal into a doublet split dependent on orientation and degree of motion [16].

Examples of spectra obtained with PSM-d₃₁, an analog of PSM with ²H substituted for ¹H at every position in the amide linked chain, mixed with CHOL and POPC or PDPC are shown in Figure 3. The spectrum with POPC has a signature shape. It is the sum of signals from all chain segments, each of which is a powder pattern comprised of a superposition of doublets from all orientations of membrane. The resultant spectrum has sharp edges and peaks within on both sides that have progressively smaller splitting due to a gradient of decreasing order along the chain towards the terminal methyl groups in the middle of the bilayer. When monounsaturated POPC is replaced by polyunsaturated PDPC, in contrast, a narrow component attributed to PSM-d₃₁ in less ordered non-raft domains superposed upon a

broader component attributed to PSM-d₃₁ in more ordered raft-like domains become resolved. Pairs of inner and outer shoulders towards the edges and of inner and outer signals near the center distinguish these features. CG simulations confirming PDPC promotes the formation of raft-like domains have been performed and will be described.

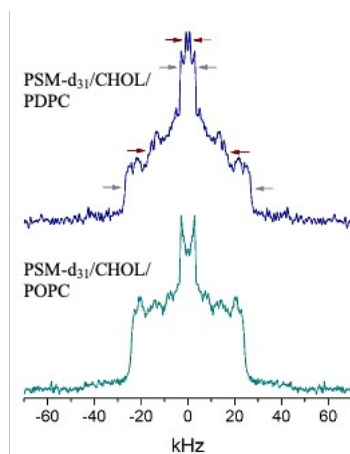


Figure 3: ^2H NMR spectra for aqueous multilamellar dispersions of PSM-d₃₁/CHOL/PDPC and PSM-d₃₁/CHOL/POPC (1:1:1 mol) at 37 °C. Arrows indicate signals attributed to raft-like (blue) and non-raft (red) domains. Adapted from [5].

4. Results

Results from two projects demonstrating analysis of CG simulations in terms of the separation of lipids into domains will be presented.

4.1 Influence of PDPC on size and formation of lipid rafts

The coarse grain (CG) simulations began with homogenously mixed bilayers composed of PSM/CHOL/POPC and PSM/CHOL/PDPC in 1:1:1 mol ratio, and PSM/CHOL/POPC/PDPC in 1:1:0.5:0.5 mol ratio. The propensity for PSM and CHOL to segregate into raft-like domains was then observed over production runs of 6 μs . Figure 4 shows snapshots of the upper leaflet after 6 μs of simulation for all three compositions of membrane. Color coded circles indicate the lateral location of PSM (red), CHOL (white), POPC (yellow) and PDPC (blue) molecules, and a color coding of areas indicates the regions

identified as raft-like (red) and non-raft (blue) according to the local concentration of lipid. The snapshots illustrate that the formation and size of PSM-rich/CHOL-rich raft-like domains is enhanced by PDPC. In PSM/CHOL/POPC, most of the bilayer remains non-raft and the domains that are PSM-rich/CHO-rich are small and few. An increase in the size of PSM-rich/CHOL-rich domains accompanies the partial replacement of POPC by PDPC in SM/CHOL/POPC/PDPC and the total substitution of POPC with PDPC in SM/CHOL/PDPC results in further increase in size.

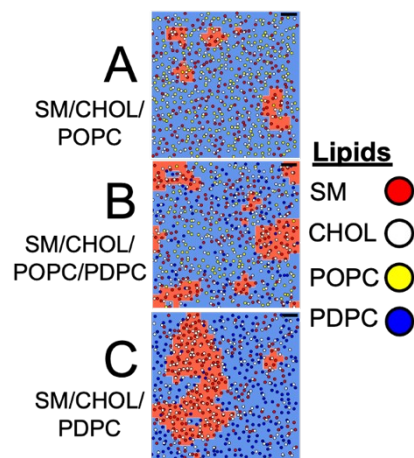


Figure 4: Top view snapshots of the upper bilayer following 6 us of simulation at 37 °C. Color coded areas indicate raft-like (red) and non-raft (blue) regions. Scale bar (black) is 2 nm.

A breakdown of the lipid content for each region averaged over the entire duration of simulation is given in Figure 5. The bar graphs provide a quantitative measure of how the amount of lipid found in PSM-rich/CHOL-rich domains is affected by PDPC. PSM-rich/CHOL-rich domains represent just 7.4% of total lipid in PSM/CHOL/POPC, rising to 16.8% in PSM/CHOL/POPC/PDPC and 34.4% in PSM/CHOL/PDPC. A minimal amount of PDPC infiltrates the PSM-rich/CHOL-rich domains. The polyunsaturated phospholipid found in the raft-like domains comprises only 0.4 and 2.3% of total lipid in

PSM/CHOL/POPC/PDPC and PSM/CHOL/PDPC, respectively. The vast majority of PDPC resides outside the PSM-rich/CHOL-rich domains in the surrounding non-raft environment.

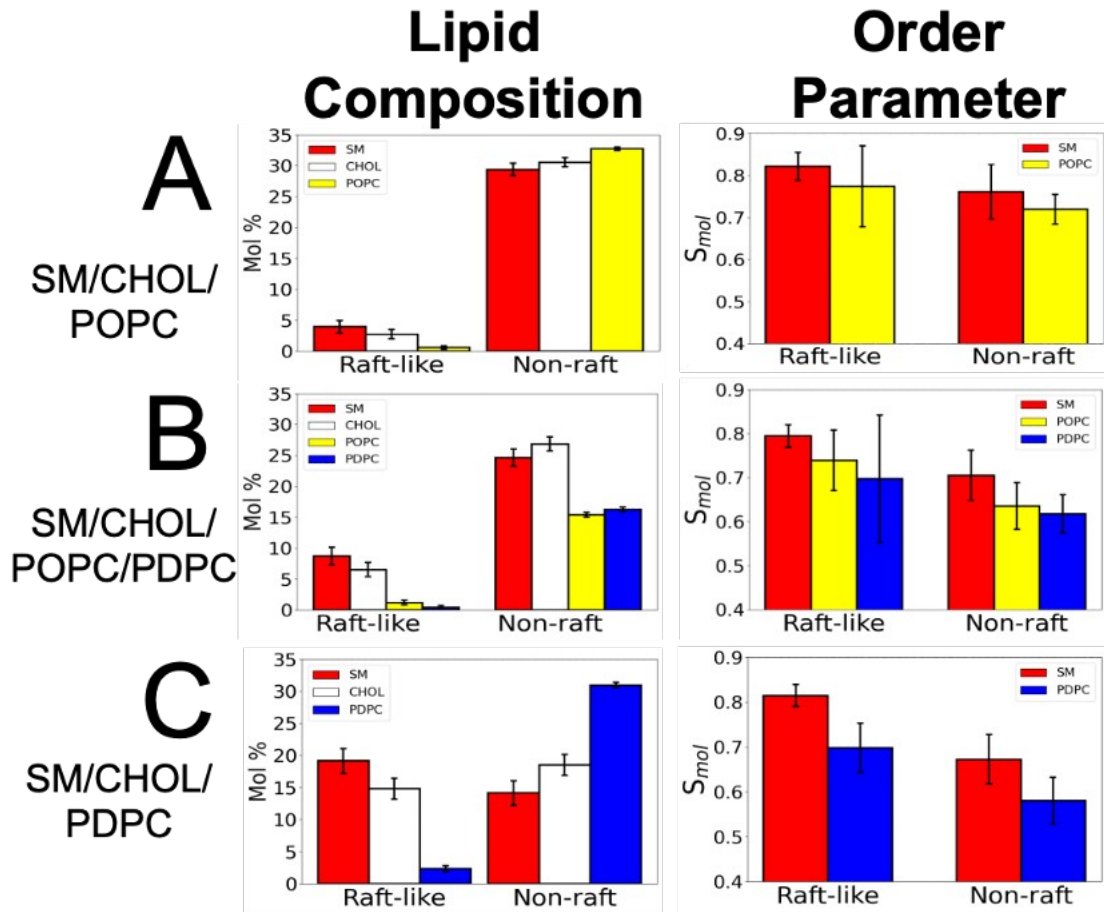


Figure 5: Composition and order parameters for lipids in raft-like and non-raft regions. Color bars designate PSM (red), CHOL (white), POPC (yellow) and PDPC (blue).

Order parameters calculated for PSM, POPC and PDPC in raft-like and non-raft environments interrogate the role that the disorder of DHA plays in determining the size of lipid rafts (Figure 5). They are defined here as

$$S_{mol} = \frac{1}{2} \langle 3 \cos^2 \theta - 1 \rangle$$

where θ is the angle that a vector connecting the first and third beads on the palmitoyl chain forms with respect to the bilayer normal and were calculated as a time and ensemble average

over the entire simulation. The bar graphs generated demonstrate that the difference in order between the two environments becomes progressively greater when POPC is partially and then entirely replaced by PDPC in the mixtures with PSM and CHOL. Greater disorder in the non-raft region where PDPC primarily locates is responsible. The non-raft value of S_{mol} (expressed as a population weighted average of the order parameters for PSM, POPC and PDPC) drops from 0.758 in PSM/CHOL/POPC to 0.680 in PSM/CHOL/POPC/PDPC and then to 0.610 in PSM/CHOL/PDPC. In contrast, there is only marginal variation in the corresponding values of S_{mol} (0.815, 0.785 and 0.803) in the raft-like domain.

The simulations are consistent with the larger size for PSM-rich/CHOL-rich domains inferred from the observation of two spectral components with deuterated analogs of PSM, PDPC and CHOL in ^2H NMR spectra when PDPC replaces POPC in mixtures with PSM and CHOL [17]. They reveal the incorporation of highly disordered PDPC into the non-raft region leads to an increase in the difference in order between raft-like and non-raft environments. We attribute the growth in size of raft-like domains to this mechanism, which supports the proposal that a tuning of membrane order underlies the health benefits of n-3 PUFA [18].

This work is part of a study submitted for publication [13]

4.2 *Lateral location of vitamin E in membranes*

The proposal that αtoc colocalizes with PDPC to optimize protection against oxidation [8] was tested in preliminary CG simulations performed on a bilayer composed PSM, CHOL, PDPC and αtoc (7:7:7:1 mol). The simulations began with a homogenously bilayer that quickly became heterogeneously mixed during a production run over 30 μs . To analyze where αtoc prefers to locate we switched from a two-state (raft-like and non-raft) to three-state (raft-like, mixed and non-raft) model. PSM-rich/CHOL-rich and PDPC-rich

regions were designated raft-like and non-raft, respectively, while elsewhere was deemed homogeneously mixed.

A representative snapshot showing a top view of the bilayer after 20 μ s of simulation illustrating the separation into domains that evolves is shown in Figure 6. Color coded circles indicate the lateral location of PSM (red), CHOL (white), PDPC (blue) and α toc (orange) molecules, and a color coding of areas indicates the regions identified as raft-like (red), non-raft (blue) and mixed (white). Visual inspection reveals α toc prefers the mixed and non-raft regions where PDPC is primarily found and is largely excluded from the raft-like region that is depleted in PDPC. The breakdown of the lipid content for each region averaged over the entire duration of simulation that is also given in Figure 6 confirms the assessment made by eye.

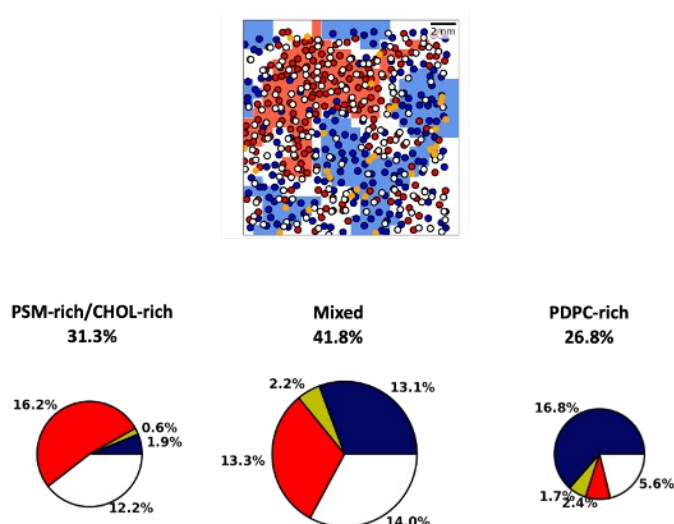


Figure 6: Top view snapshot of the upper bilayer following 20 μ s of simulation for PSM/CHOL/PDPC/ α toc at 37 $^{\circ}$ C (upper panel). Color coded areas indicate raft-like (red), non-raft (blue) and mixed (white) regions. Composition of lipids (relative to total lipid) in raft-like, non-raft and mixed regions (lower panel). Colored segments in the pie graph designate PSM (red), CHOL (white), PDPC (blue) and α toc (yellow).

The simulations, however, must be considered preliminary. A CG representation for the structure of α toc does not exist in the Martini database. In earlier work from another group a model was constructed with a saturated chain for the branched side chain [19]. Our

model was created inhouse with beads that typically represent an unsaturated chain to better resemble the properties of a branched side chain. Comparison with all-atom (AA) simulations suggests that the sidechain modeled is too disordered and models with less unsaturation will be tried to better capture molecular organization.

References

1. Stillwell, W. 2015. An Introduction to Biological Membranes: Composition, Structure and Function, 2nd ed., Elsevier, Amsterdam.
2. Levental, I, Levental, K. and Heberle, F.A. 2020. Trends in Cell Biology 30:341-353
3. Marques-da-Silva, Dorinda, and Ricardo Lagoa. "Rafting on the Evidence for Lipid Raft-like Domains as Hubs Triggering Environmental Toxicants' Cellular Effects." Molecules 28.18 (2023): 6598.
4. Calder, P.C. 2020. *n*-3 PUFA and inflammation: from membrane to nucleus and from bench to bedside. Proc. Nutr. Soc. 79, 404–416.
5. Wassall, S.R., Leng, X., Canner, S.W., Pennington, E.R., Kinnun, J.J., Cavazos, A.T., Dadoo, S., Johnson, D., Heberle, F.A., Katsaras, J. and Shaikh, S.R. 2018. Docosahexaenoic acid regulates the formation of lipid rafts: A unified view from experiment and simulation. Biochim. Biophys. Acta 1860, 1985-1993.
6. Niki, E. and Abe, K. Vitamin E: structure, properties and functions. 2019. In Vitamin E: Chemistry and Nutritional Benefits; Niki, E., Ed.; The Royal Society of Chemistry, London, pp. 1-11.
7. Atkinson, J., Epand, R.F. and Epand, R.M. 2008. Tocopherols and tocotrienols in membranes: a critical review. Free Rad. Biol. Med. 44, 739-764.

8. Zhong, S. and Yin, H. 2019. Lipid peroxidation: role of vitamin E. In *Vitamin E: Chemistry and Nutritional Benefits*; Niki, E., Ed.; The Royal Society of Chemistry, London, pp. 118-134.
9. Atkinson, J., Harroun, T., Wassall, S.R. Stillwell, W. and Katsaras, J. 2010. The location and behavior of α -tocopherol in membranes. *Mol. Nutr. Food Res.* 54, 641-651.
10. Shaikh, S.R., Kinnun, J.J., Leng, X., Williams, J.A. and Wassall, S.R. 2015. How polyunsaturated fatty acids modify molecular organization in membranes: Insight from NMR studies of model systems. *Biochim. Biophys. Acta* 1848, 211-219.
11. Kimble-Hill, A.C., Petrache, H.I., Seifert, S. and Firestone, M.A. 2018. Reorganization of ternary lipid mixtures of nonphosphorylated phosphatidylinositol interacting with angiomin. *J. Phys. Chem. B* 122, 8404-8415.
12. Marrink, S.J., Risselada, H.J., Yefimov, S., Tieleman, D.P. and De Vries, A.H. 2007. The martini force field: coarse grained model for biomolecular simulations. *J. Phys. Chem. B*, 111, 7812–7824.
13. E. Pennington, M. Bridges, R. Virk, B. Bathon, N. Beatty, R. Gray, P. Kelley, S. Wassall, J. Manke, N. Reisdorph, J. Fenton, K. Gowdy, and S. Shaikh. Docosahexaenoic acid controls pulmonary macrophage lipid raft size and inflammation. *J. Nutrition*, *submitted*.
14. Hess, B.; Kutzner, C.; van der Spoel, D.; Lindahl, E. GROMACS 4: Algorithms for highly efficient, load-balanced, and scalable molecular simulation. *J. Chem. Theory Comput.* 2008, 4, 435-447.
15. Cavazos, Andres T., et al. "OxPAPC stabilizes liquid-ordered domains in biomimetic membranes." *Biophysical Journal* 122.6 (2023): 1130-1139.
16. Seelig, Joachim. "Deuterium magnetic resonance: theory and application to lipid membranes." *Quarterly reviews of biophysics* 10.3 (1977): 353-418.

17. Kinnun, Jacob J., et al. "DHA modifies the size and composition of raftlike domains: a solid-state ^2H NMR study." *Biophysical Journal* 114.2 (2018): 380-391.
18. Levental, Kandice R., et al. "Polyunsaturated lipids regulate membrane domain stability by tuning membrane order." *Biophysical journal* 110.8 (2016): 1800-1810.
19. Muddana, Hari S., Homer H. Chiang, and Peter J. Butler. "Tuning membrane phase separation using nonlipid amphiphiles." *Biophysical journal* 102.3 (2012): 489-497.